Northumbria Research Link

A quasi-3D hyperbolic shear deformation theory for functionally graded plates

Huu-Tai Thai [a,*], Thuc P. Vo [b], Tinh Q. Bui [c], Trung-Kien Nguyen [d]

[a] School of Civil and Environmental Engineering, The University of New South Wales, Sydney, Australia

[b] Faculty of Engineering and Environment, Northumbria University, Newcastle upon Tyne, NE1 8ST, UK.

[c] Department of Civil Engineering, University of Siegen, Paul-Bonatz-Str. 9-11, 57076, Siegen, Germany.

[d] Faculty of Civil Engineering and Applied Mechanics, University of Technical Education Ho Chi Minh City, 1 Vo Van Ngan Street, Thu Duc District, Ho Chi Minh City, Vietnam

Abstract

A quasi-3D hyperbolic shear deformation theory for functionally graded plates is developed. The theory accounts for both shear deformation and thickness stretching effects by a hyperbolic variation of all displacements across the thickness, and satisfies the stress-free boundary conditions on the top and bottom surfaces of the plate without requiring any shear correction factor. The benefit of the present theory is that it contains less number of unknowns and governing equations than the existing quasi-3D theories, but its solutions are compared well with 3D and quasi-3D solutions. Equations of motion are derived from Hamilton principle. Analytical solutions for bending and free vibration problems are obtained for simply supported plates. Numerical examples are presented to verify the accuracy of the present theory.

[*] Corresponding author. Tel.: + 82 2 2220 4154.
E-mail address: thaihuutai@hanyang.ac.kr (H.T. Thai).

1. Introduction

Functionally graded materials (FGMs) are a type of nonhomogeneous composites materials, in which the material properties vary smoothly and continuously from one surface to another. A typical FGM is made from a mixture of two material phases, for example, a ceramic and a metal. An advantage of FGMs over laminated composites is that it eliminates the delamination mode of failure found in the laminated composites. In addition, the material properties of FGMs can be tailored to different applications and working environments. This makes FGMs preferable in many structural applications such as nuclear reactor, aerospace, mechanical, automotive, and civil engineering.

Since the shear deformation effects are more pronounced in advanced composites like FGMs, shear deformation theories such as first-order shear deformation theory (FSDT) and higher-order shear deformation theories (HSDTs) should be used. The FSDT [1-9] gives acceptable prediction, but requires a shear correction factor which is hard to find out consistently because of dependent on many parameters including geometry, boundary conditions, and loading conditions. The HSDTs [10-17] do not require a shear correction factor, but their equations of motion are more complicated than those of the FSDT. It should be noted that the thickness stretching effect (i.e., $\varepsilon_z = 0$) is ignored in both the FSDT and HSDTs by assuming a constant transverse displacement through the thickness of the plate. Although this assumption is appropriate for moderately thick functionally graded (FG) plates, but is inaccurate for thick FG ones [18]. The importance of the thickness stretching effect in FG plates has been pointed out in the work of Carrera et al. [19].

Quasi-3D theories are HSDTs in which the transverse displacement is expanded as a higher-order variation through the thickness of the plate, and hence, thickness stretching

effect is captured. There are several quasi-3D theories proposed in the literature. For example, Kant and Swaminathan [20] proposed a quasi-3D theory with all displacement components expanded as a cubic variation through the thickness. The theories presented by Chen et al. [21], Talha and Singh [22], Reddy [23], and Neves et al. [24] are based on a cubic variation of in-plane displacements and a quadratic variation of transverse displacement. Instead of using polynomial functions, Ferreira et al. [25] employed the sinusoidal functions for all displacement components. Neves et al. [26-27] employed the polynomial and the non-polynomial (sinusoidal [26] and hyperbolic [27]) functions for transverse and in-plane displacements, respectively. It should be noted that the above-mentioned quasi-3D theories are too cumbersome and computationally expensive since they handle many unknowns (e.g., theories by Ref. [20] with twelve unknowns, Refs. [21-23] with eleven unknowns, and Refs. [25-27,24] with nine unknowns). Recently, Mantari and Guedes Soares [28] presented a generalized formulation in which many hybrid quasi-3D theories with six unknowns can be derived. Although the hybrid quasi-3D theories [28] have six unknowns, they are still more complicated than the FSDT. As a consequence, a simple quasi-3D theory proposed in the present work is necessary.

This work aims to develop a simple quasi-3D theory with only five unknowns for bending and free vibration analysis of FG plates. The displacement field is chosen based on a generalized formulation [28] with a hyperbolic variation for all displacements. By dividing the transverse displacement into the bending and shear parts, the number of unknowns of the theory is reduced, and thus saving computational time. Equations of motion derived from Hamilton principle are analytically solved for bending and free vibration problems of a simply supported plate. Numerical examples are presented to verify the accuracy of the present theory.

2. Theoretical formulation

As mentioned above, the displacement field of the present theory is chosen based on the generalized formulation with a hyperbolic variation for all displacement components. In fact, the use of hyperbolic functions was first proposed by Soldatos [29], later used by Xiang et al. [30], Akavci [31], and El Meiche et al. [32], and recently by Neves et al. [27]. According to Refs. [33,28], the displacement field takes the form

$$u_1(x,y,z,t) = u(x,y,t) - z\frac{\partial w}{\partial x} + \Psi(z)\varphi_x$$

$$u_2(x,y,z,t) = v(x,y,t) - z\frac{\partial w}{\partial y} + \Psi(z)\varphi_y \qquad (1)$$

$$u_3(x,y,z,t) = w(x,y,t) + \Psi'(z)\varphi_z(x,y,t)$$

where $u, v, w, \varphi_x, \varphi_y$ and φ_z are six unknown displacement functions of midplane of the plate; and $\Psi(z)$ is a shape function representing the distribution of the transvese shear strains and shear stresses through the thickness. In this study, the shape function is chosen based on the hyperbolic function proposed by Soldatos [29] as

$$\Psi(z) = h\sinh\left(\frac{z}{h}\right) - z\cosh\left(\frac{1}{2}\right) \qquad (2)$$

with h being the thickness of the plate. By deviding the transverse displacement w into bending and shear parts (i.e., $w = w_b + w_s$) and making further assumptions given by $\varphi_x = \partial w_s/\partial x$ and $\varphi_y = \partial w_s/\partial y$, the displacement field of the present theory can be rewritten in simpler form as

$$u_1(x,y,z,t) = u(x,y,t) - z\frac{\partial w_b}{\partial x} - f(z)\frac{\partial w_s}{\partial x}$$

$$u_2(x,y,z,t) = v(x,y,t) - z\frac{\partial w_b}{\partial y} - f(z)\frac{\partial w_s}{\partial y} \qquad (3)$$

$$u_3(x,y,z,t) = w_b(x,y,t) + w_s(x,y,t) + g(z)\varphi_z(x,y,t)$$

where $f(z) = z - \Psi(z)$ and $g(z) = \Psi'(z) = 1 - f'(z) = \cosh(z/h) - \cosh(1/2)$.

Clearly seen that the displacement field in Eq. (3) handles only five unknowns, i.e., $u, v, w_b, w_s, \varphi_z$.

The strains associated with the displacement field in Eq. (3) are:

$$\varepsilon_x = \frac{\partial u}{\partial x} - z\frac{\partial^2 w_b}{\partial x^2} - f(z)\frac{\partial^2 w_s}{\partial x^2} \tag{4a}$$

$$\varepsilon_y = \frac{\partial v}{\partial y} - z\frac{\partial^2 w_b}{\partial y^2} - f(z)\frac{\partial^2 w_s}{\partial y^2} \tag{4b}$$

$$\varepsilon_z = g'(z)\varphi_z \tag{4c}$$

$$\gamma_{xy} = \frac{\partial u}{\partial y} + \frac{\partial v}{\partial x} - 2z\frac{\partial^2 w_b}{\partial x\partial y} - 2f(z)\frac{\partial^2 w_s}{\partial x\partial y} \tag{4d}$$

$$\gamma_{xz} = g(z)\left(\frac{\partial w_s}{\partial x} + \frac{\partial \varphi_z}{\partial x}\right) \tag{4e}$$

$$\gamma_{yz} = g(z)\left(\frac{\partial w_s}{\partial y} + \frac{\partial \varphi_z}{\partial y}\right) \tag{4f}$$

It can be seen from Eqs. (4e) and (4f) that the transverse shear strains $(\gamma_{xz}, \gamma_{yz})$ are equal to zero at the top ($z = h/2$) and bottom ($z = -h/2$) surfaces of the plate. A shear correction factor is, therefore, not required.

The constitutive relations of a FG plate can be written as

$$\begin{Bmatrix} \sigma_x \\ \sigma_y \\ \sigma_z \\ \sigma_{xy} \\ \sigma_{xz} \\ \sigma_{yz} \end{Bmatrix} = \begin{bmatrix} C_{11} & C_{12} & C_{13} & 0 & 0 & 0 \\ C_{12} & C_{22} & C_{23} & 0 & 0 & 0 \\ C_{13} & C_{23} & C_{33} & 0 & 0 & 0 \\ 0 & 0 & 0 & C_{66} & 0 & 0 \\ 0 & 0 & 0 & 0 & C_{55} & 0 \\ 0 & 0 & 0 & 0 & 0 & C_{44} \end{bmatrix} \begin{Bmatrix} \varepsilon_x \\ \varepsilon_y \\ \varepsilon_z \\ \gamma_{xy} \\ \gamma_{xz} \\ \gamma_{yz} \end{Bmatrix} \tag{5}$$

where C_{ij} are the three-dimensional elastic constants determined by

$$C_{11} = C_{22} = C_{33} = \frac{(1-\nu)E}{(1-2\nu)(1+\nu)} \tag{6a}$$

$$C_{12} = C_{13} = C_{23} = \frac{\nu E}{(1-2\nu)(1+\nu)} \tag{6b}$$

$$C_{44} = C_{55} = C_{66} = \frac{E}{2(1+\nu)} \tag{6c}$$

with E and ν being Young's modulus and Poisson's ratio, respectively, of a FG plate.

Hamilton's principle is used herein to derive the equations of motion. The principle can be stated in analytical form as

$$\int_0^T (\delta U + \delta V - \delta K) dt = 0 \tag{7}$$

where δU is the variation of strain energy; δV is the variation of work done by external forces; and δK is the variation of kinetic energy.

The variation of strain energy is given explicitly by

$$
\begin{aligned}
\delta U &= \int_A \int_{-h/2}^{h/2} \left(\sigma_x \delta \varepsilon_x + \sigma_y \delta \varepsilon_y + \sigma_z \delta \varepsilon_z + \sigma_{xy} \delta \gamma_{xy} + \sigma_{xz} \delta \gamma_{xz} + \sigma_{yz} \delta \gamma_{yz} \right) dA dz \\
&= \int_A \left[N_x \frac{\partial \delta u}{\partial x} - M_x \frac{\partial^2 \delta w_b}{\partial x^2} - P_x \frac{\partial^2 \delta w_s}{\partial x^2} + N_y \frac{\partial \delta v}{\partial y} - M_y \frac{\partial^2 \delta w_b}{\partial y^2} - P_y \frac{\partial^2 \delta w_s}{\partial y^2} \right. \\
&\quad + R_z \delta \varphi_z + N_{xy} \left(\frac{\partial \delta u}{\partial y} + \frac{\partial \delta v}{\partial x} \right) - 2M_{xy} \frac{\partial^2 \delta w_b}{\partial x \partial y} - 2P_{xy} \frac{\partial^2 \delta w_s}{\partial x \partial y} \\
&\quad \left. + Q_x \left(\frac{\partial \delta w_s}{\partial x} + \frac{\partial \delta \varphi_z}{\partial x} \right) + Q_y \left(\frac{\partial \delta w_s}{\partial y} + \frac{\partial \delta \varphi_z}{\partial y} \right) \right] dA
\end{aligned}
\tag{8}
$$

where N, M, P, Q, and R are the stress resultants defined by

$$\left(N_x, N_y, N_{xy} \right) = \int_{-h/2}^{h/2} \left(\sigma_x, \sigma_y, \sigma_{xy} \right) dz \tag{9a}$$

$$\left(M_x, M_y, M_{xy} \right) = \int_{-h/2}^{h/2} \left(\sigma_x, \sigma_y, \sigma_{xy} \right) z dz \tag{9b}$$

6

$$\left(P_x, P_y, P_{xy}\right) = \int_{-h/2}^{h/2} \left(\sigma_x, \sigma_y, \sigma_{xy}\right) f(z) dz \tag{9c}$$

$$\left(Q_x, Q_y\right) = \int_{-h/2}^{h/2} \left(\sigma_{xz}, \sigma_{yz}\right) g(z) dz \tag{9d}$$

$$R_z = \int_{-h/2}^{h/2} \sigma_z g'(z) dz \tag{9e}$$

Substituting Eq. (4) into Eq. (5) and the subsequent results into Eq. (9), the stress resultants can be expressed in terms of generalized displacements $\left(u, v, w_b, w_s, \varphi_z\right)$ as

$$\begin{Bmatrix} N_x \\ N_y \\ N_{xy} \\ M_x \\ M_y \\ M_{xy} \\ P_x \\ P_y \\ P_{xy} \\ R_z \end{Bmatrix} = \begin{bmatrix} A_{11} & A_{12} & 0 & B_{11} & B_{12} & 0 & B_{11}^s & B_{12}^s & 0 & X_{13} \\ A_{12} & A_{22} & 0 & B_{12} & B_{22} & 0 & B_{12}^s & B_{22}^s & 0 & X_{23} \\ 0 & 0 & A_{66} & 0 & 0 & B_{66} & 0 & 0 & B_{66}^s & 0 \\ B_{11} & B_{12} & 0 & D_{11} & D_{12} & 0 & D_{11}^s & D_{12}^s & 0 & Y_{13} \\ B_{12} & B_{22} & 0 & D_{12} & D_{22} & 0 & D_{12}^s & D_{22}^s & 0 & Y_{23} \\ 0 & 0 & B_{66} & 0 & 0 & D_{66} & 0 & 0 & D_{66}^s & 0 \\ B_{11}^s & B_{12}^s & 0 & D_{11}^s & D_{12}^s & 0 & H_{11} & H_{12} & 0 & Y_{13}^s \\ B_{12}^s & B_{22}^s & 0 & D_{12}^s & D_{22}^s & 0 & H_{12} & H_{22} & 0 & Y_{23}^s \\ 0 & 0 & B_{66}^s & 0 & 0 & D_{66}^s & 0 & 0 & H_{66} & 0 \\ X_{13} & X_{23} & 0 & Y_{13} & Y_{23} & 0 & Y_{13}^s & Y_{23}^s & 0 & Z_{33} \end{bmatrix} \begin{Bmatrix} \frac{\partial u}{\partial x} \\ \frac{\partial v}{\partial y} \\ \frac{\partial u}{\partial y} + \frac{\partial v}{\partial x} \\ -\frac{\partial^2 w_b}{\partial x^2} \\ -\frac{\partial^2 w_b}{\partial y^2} \\ -2\frac{\partial^2 w_b}{\partial x \partial x} \\ -\frac{\partial^2 w_s}{\partial x^2} \\ -\frac{\partial^2 w_s}{\partial y^2} \\ -2\frac{\partial^2 w_s}{\partial x \partial y} \\ \varphi_z \end{Bmatrix} \tag{10a}$$

$$\begin{Bmatrix} Q_x \\ Q_y \end{Bmatrix} = \begin{bmatrix} A_{55}^s & 0 \\ 0 & A_{44}^s \end{bmatrix} \begin{Bmatrix} \frac{\partial w_s}{\partial x} + \frac{\partial \varphi_z}{\partial x} \\ \frac{\partial w_s}{\partial y} + \frac{\partial \varphi_z}{\partial y} \end{Bmatrix} \tag{10b}$$

where

$$\left(A_{ij}, A_{ij}^s, B_{ij}, B_{ij}^s, D_{ij}, D_{ij}^s, H_{ij}\right) = \int_{-h/2}^{h/2} \left(1, g^2, z, f, z^2, fz, f^2\right) C_{ij} dz \tag{11a}$$

$$\left(X_{ij}, Y_{ij}, Y_{ij}^s, Z_{ij}\right) = \int_{-h/2}^{h/2} \left(1, z, f, g'\right) g' C_{ij} dz \tag{11b}$$

The variation of work done by externally transverse loads q can be expressed as

7

$$\delta V = -\int_A q\delta\left(w_b + w_s + g\varphi_z\right)dA \tag{12}$$

The variation of kinetic energy is

$$\delta K = \int_A \int_{-h/2}^{h/2} \rho\left(\dot{u}_1\delta\dot{u}_1 + \dot{u}_2\delta\dot{u}_2 + \dot{u}_3\delta\dot{u}_3\right)dAdz$$

$$= \int_A \left\{ I_0\left[\dot{u}\delta\dot{u} + \dot{v}\delta\dot{v} + \left(\dot{w}_b + \dot{w}_s\right)\delta\left(\dot{w}_b + \dot{w}_s\right)\right] + J_0\left[\left(\dot{w}_b + \dot{w}_s\right)\delta\dot{\varphi}_z + \dot{\varphi}_z\delta\left(\dot{w}_b + \dot{w}_s\right)\right] \right.$$

$$- I_1\left(\dot{u}\frac{\partial\delta\dot{w}_b}{\partial x} + \frac{\partial\dot{w}_b}{\partial x}\delta\dot{u} + \dot{v}\frac{\partial\delta\dot{w}_b}{\partial y} + \frac{\partial\dot{w}_b}{\partial y}\delta\dot{v}\right) + I_2\left(\frac{\partial\dot{w}_b}{\partial x}\frac{\partial\delta\dot{w}_b}{\partial x} + \frac{\partial\dot{w}_b}{\partial y}\frac{\partial\delta\dot{w}_b}{\partial y}\right) \tag{13}$$

$$- J_1\left(\dot{u}\frac{\partial\delta\dot{w}_s}{\partial x} + \frac{\partial\dot{w}_s}{\partial x}\delta\dot{u} + \dot{v}\frac{\partial\delta\dot{w}_s}{\partial y} + \frac{\partial\dot{w}_s}{\partial y}\delta\dot{v}\right) + K_2\left(\frac{\partial\dot{w}_s}{\partial x}\frac{\partial\delta\dot{w}_s}{\partial x} + \frac{\partial\dot{w}_s}{\partial y}\frac{\partial\delta\dot{w}_s}{\partial y}\right)$$

$$\left. + J_2\left(\frac{\partial\dot{w}_b}{\partial x}\frac{\partial\delta\dot{w}_s}{\partial x} + \frac{\partial\dot{w}_s}{\partial x}\frac{\partial\delta\dot{w}_b}{\partial x} + \frac{\partial\dot{w}_b}{\partial y}\frac{\partial\delta\dot{w}_s}{\partial y} + \frac{\partial\dot{w}_s}{\partial y}\frac{\partial\delta\dot{w}_b}{\partial y}\right) + K_0\dot{\varphi}_z\delta\dot{\varphi}_z \right\}dA$$

where dot-superscript convention indicates the differentiation with respect to the time variable t; ρ is the mass density; and $\left(I_i, J_i, K_i\right)$ are the mass moments of inertia defined by

$$\left(I_0, I_1, I_2\right) = \int_{-h/2}^{h/2}\left(1, z, z^2\right)\rho dz \tag{14a}$$

$$\left(J_0, J_1, J_2\right) = \int_{-h/2}^{h/2}\left(g, f, fz\right)\rho dz \tag{14b}$$

$$\left(K_0, K_2\right) = \int_{-h/2}^{h/2}\left(g^2, f^2\right)\rho dz \tag{14c}$$

The equations of motion can be obtained by substituting the expressions for δU, δV, and δK from Eqs. (8), (12), and (13) into Eq. (7), integrating by parts, and collecting the coefficients of δu, δv, δw_b, δw_s, and $\delta\varphi_z$.

$$\delta u: \ \frac{\partial N_x}{\partial x} + \frac{\partial N_{xy}}{\partial y} = I_0\ddot{u} - I_1\frac{\partial\ddot{w}_b}{\partial x} - J_1\frac{\partial\ddot{w}_s}{\partial x} \tag{15a}$$

$$\delta v: \ \frac{\partial N_{xy}}{\partial x} + \frac{\partial N_y}{\partial y} = I_0\ddot{v} - I_1\frac{\partial\ddot{w}_b}{\partial y} - J_1\frac{\partial\ddot{w}_s}{\partial y} \tag{15b}$$

$$\delta w_b : \frac{\partial^2 M_x}{\partial x^2} + 2\frac{\partial^2 M_{xy}}{\partial x \partial y} + \frac{\partial^2 M_y}{\partial y^2} + q$$

$$= I_0\left(\ddot{w}_b + \ddot{w}_s\right) + J_0\ddot{\varphi}_z + I_1\left(\frac{\partial \ddot{u}}{\partial x} + \frac{\partial \ddot{v}}{\partial y}\right) - I_2\nabla^2\ddot{w}_b - J_2\nabla^2\ddot{w}_s \tag{15c}$$

$$\delta w_s : \frac{\partial^2 P_x}{\partial x^2} + 2\frac{\partial^2 P_{xy}}{\partial x \partial y} + \frac{\partial^2 P_y}{\partial y^2} + \frac{\partial Q_x}{\partial x} + \frac{\partial Q_y}{\partial y} + q$$

$$= I_0\left(\ddot{w}_b + \ddot{w}_s\right) + J_0\ddot{\varphi}_z + J_1\left(\frac{\partial \ddot{u}}{\partial x} + \frac{\partial \ddot{v}}{\partial y}\right) - J_2\nabla^2\ddot{w}_b - K_2\nabla^2\ddot{w}_s \tag{15d}$$

$$\delta\varphi_z : \frac{\partial Q_x}{\partial x} + \frac{\partial Q_y}{\partial y} - R_z + gq = J_0\left(\ddot{w}_b + \ddot{w}_s\right) + K_0\ddot{\varphi}_z \tag{15e}$$

Substituting Eq. (10) into Eq. (15), the equations of motion of the present theory can be expressed in terms of displacements $\left(u, v, w_b, w_s, \varphi_z\right)$ as

$$A_{11}\frac{\partial^2 u}{\partial x^2} + A_{66}\frac{\partial^2 u}{\partial y^2} + \left(A_{12} + A_{66}\right)\frac{\partial^2 v}{\partial x \partial y} - B_{11}\frac{\partial^3 w_b}{\partial x^3} - \left(B_{12} + 2B_{66}\right)\frac{\partial^3 w_b}{\partial x \partial y^2}$$

$$-B_{11}^s\frac{\partial^3 w_s}{\partial x^3} - \left(B_{12}^s + 2B_{66}^s\right)\frac{\partial^3 w_s}{\partial x \partial y^2} + X_{13}\frac{\partial \varphi_z}{\partial x} = I_0\ddot{u} - I_1\frac{\partial \ddot{w}_b}{\partial x} - J_1\frac{\partial \ddot{w}_s}{\partial x} \tag{16a}$$

$$A_{22}\frac{\partial^2 v}{\partial y^2} + A_{66}\frac{\partial^2 v}{\partial x^2} + \left(A_{12} + A_{66}\right)\frac{\partial^2 u}{\partial x \partial y} - B_{22}\frac{\partial^3 w_b}{\partial y^3} - \left(B_{12} + 2B_{66}\right)\frac{\partial^3 w_b}{\partial x^2 \partial y}$$

$$-B_{22}^s\frac{\partial^3 w_s}{\partial y^3} - \left(B_{12}^s + 2B_{66}^s\right)\frac{\partial^3 w_s}{\partial x^2 \partial y} + X_{23}\frac{\partial \varphi_z}{\partial y} = I_0\ddot{v} - I_1\frac{\partial \ddot{w}_b}{\partial y} - J_1\frac{\partial \ddot{w}_s}{\partial y} \tag{16b}$$

$$B_{11}\frac{\partial^3 u}{\partial x^3} + \left(B_{12} + 2B_{66}\right)\left(\frac{\partial^3 u}{\partial x \partial y^2} + \frac{\partial^3 v}{\partial x^2 \partial y}\right) + B_{22}\frac{\partial^3 v}{\partial y^3} - D_{11}\frac{\partial^4 w_b}{\partial x^4} - D_{22}\frac{\partial^4 w_b}{\partial y^4}$$

$$-2\left(D_{12} + 2D_{66}\right)\frac{\partial^4 w_b}{\partial x^2 \partial y^2} - D_{11}^s\frac{\partial^4 w_s}{\partial x^4} - D_{22}^s\frac{\partial^4 w_s}{\partial y^4} - 2\left(D_{12}^s + 2D_{66}^s\right)\frac{\partial^4 w_s}{\partial x^2 \partial y^2} \tag{16c}$$

$$+Y_{13}\frac{\partial^2 \varphi_z}{\partial x^2} + Y_{23}\frac{\partial^2 \varphi_z}{\partial y^2} + q = I_0\left(\ddot{w}_b + \ddot{w}_s\right) + J_0\ddot{\varphi}_z + I_1\left(\frac{\partial \ddot{u}}{\partial x} + \frac{\partial \ddot{v}}{\partial y}\right) - I_2\nabla^2\ddot{w}_b - J_2\nabla^2\ddot{w}_s$$

$$B_{11}^s \frac{\partial^3 u}{\partial x^3} + \left(B_{12}^s + 2B_{66}^s\right)\left(\frac{\partial^3 u}{\partial x \partial y^2} + \frac{\partial^3 v}{\partial x^2 \partial y}\right) + B_{22}^s \frac{\partial^3 v}{\partial y^3} - D_{11}^s \frac{\partial^4 w_b}{\partial x^4} - D_{22}^s \frac{\partial^4 w_b}{\partial y^4}$$

$$-2\left(D_{12}^s + 2D_{66}^s\right)\frac{\partial^4 w_b}{\partial x^2 \partial y^2} - H_{11} \frac{\partial^4 w_s}{\partial x^4} - H_{22} \frac{\partial^4 w_s}{\partial y^4} - 2\left(H_{12} + 2H_{66}\right)\frac{\partial^4 w_s}{\partial x^2 \partial y^2}$$

$$+A_{55}^s \frac{\partial^2 w_s}{\partial x^2} + A_{44}^s \frac{\partial^2 w_s}{\partial y^2} + \left(Y_{13}^s + A_{55}^s\right)\frac{\partial^2 \varphi_z}{\partial x^2} + \left(Y_{23}^s + A_{44}^s\right)\frac{\partial^2 \varphi_z}{\partial y^2} + q \qquad (16d)$$

$$= I_0\left(\ddot{w}_b + \ddot{w}_s\right) + J_0 \ddot{\varphi}_z + J_1\left(\frac{\partial \ddot{u}}{\partial x} + \frac{\partial \ddot{v}}{\partial y}\right) - J_2 \nabla^2 \ddot{w}_b - K_2 \nabla^2 \ddot{w}_s$$

$$-X_{13} \frac{\partial u}{\partial x} - X_{23} \frac{\partial v}{\partial y} + Y_{13} \frac{\partial^2 w_b}{\partial x^2} + Y_{23} \frac{\partial^2 w_b}{\partial y^2} + \left(Y_{13}^s + A_{55}^s\right)\frac{\partial^2 w_s}{\partial x^2} + \left(Y_{23}^s + A_{44}^s\right)\frac{\partial^2 w_s}{\partial y^2}$$

$$+A_{55}^s \frac{\partial^2 \varphi_z}{\partial x^2} + A_{44}^s \frac{\partial^2 \varphi_z}{\partial y^2} - Z_{33}\varphi_z + gq = J_0\left(\ddot{w}_b + \ddot{w}_s\right) + K_0 \ddot{\varphi}_z \qquad (16e)$$

3. Analytical solutions

Consider a simply supported rectangular plate with length a and width b under transverse load q. Based on Navier solution method, the following expansions of displacements $\left(u, v, w_b, w_s, \varphi_z\right)$ are assumed as

$$u(x, y, t) = \sum_{m=1}^{\infty} \sum_{n=1}^{\infty} U_{mn} e^{i\omega t} \cos \alpha x \sin \beta y$$

$$v(x, y, t) = \sum_{m=1}^{\infty} \sum_{n=1}^{\infty} V_{mn} e^{i\omega t} \sin \alpha x \cos \beta y$$

$$w_b(x, y, t) = \sum_{m=1}^{\infty} \sum_{n=1}^{\infty} W_{bmn} e^{i\omega t} \sin \alpha x \sin \beta y \qquad (17)$$

$$w_s(x, y, t) = \sum_{m=1}^{\infty} \sum_{n=1}^{\infty} W_{smn} e^{i\omega t} \sin \alpha x \sin \beta y$$

$$\varphi_z(x, y, t) = \sum_{m=1}^{\infty} \sum_{n=1}^{\infty} \phi_{zmn} e^{i\omega t} \sin \alpha x \sin \beta y$$

where $i = \sqrt{-1}$, $\alpha = m\pi/a$, $\beta = n\pi/b$, $\left(U_{mn}, V_{mn}, W_{bmn}, W_{smn}, \phi_{zmn}\right)$ are the unknown maximum displacement coefficients, and ω is the vibration frequency. The transverse load q is also expanded as

$$q(x,y) = \sum_{m=1}^{\infty} \sum_{n=1}^{\infty} Q_{mn} \sin \alpha x \sin \beta y \tag{18}$$

For the case of sinusoidal load, coefficient $Q_{mn} = q_0$ represents the intensity of the load at the plate center. Substituting Eqs. (17) and (18) into Eq. (16), the analytical solutions can be obtained by

$$\left(\begin{bmatrix} k_{11} & k_{12} & k_{13} & k_{14} & k_{15} \\ k_{12} & k_{22} & k_{23} & k_{24} & k_{25} \\ k_{13} & k_{23} & k_{33} & k_{34} & k_{35} \\ k_{14} & k_{24} & k_{34} & k_{44} & k_{45} \\ k_{15} & k_{25} & k_{35} & k_{45} & k_{55} \end{bmatrix} - \omega^2 \begin{bmatrix} m_{11} & 0 & m_{13} & m_{14} & 0 \\ 0 & m_{22} & m_{23} & m_{24} & 0 \\ m_{13} & m_{23} & m_{33} & m_{34} & m_{35} \\ m_{14} & m_{24} & m_{34} & m_{44} & m_{45} \\ 0 & 0 & m_{35} & m_{45} & m_{55} \end{bmatrix} \right) \begin{Bmatrix} U_{mn} \\ V_{mn} \\ W_{bmn} \\ W_{smn} \\ \phi_{zmn} \end{Bmatrix} = \begin{Bmatrix} 0 \\ 0 \\ Q_{mn} \\ Q_{mn} \\ 0 \end{Bmatrix} \tag{19}$$

where

$$k_{11} = A_{11}\alpha^2 + A_{66}\beta^2, \ k_{22} = A_{66}\alpha^2 + A_{22}\beta^2, \ k_{12} = (A_{12} + A_{66})\alpha\beta,$$
$$k_{13} = -B_{11}\alpha^3 - (B_{12} + 2B_{66})\alpha\beta^2, \ k_{14} = -B_{11}^s\alpha^3 - (B_{12}^s + 2B_{66}^s)\alpha\beta^2, \ k_{15} = -X_{13}\alpha$$
$$k_{23} = -B_2\beta^3 - (B_{12} + 2B_{66})\alpha^2\beta, \ k_{24} = -B_{22}^s\beta^3 - (B_{12}^s + 2B_{66}^s)\alpha^2\beta, \ k_{25} = -X_{23}\beta$$
$$k_{33} = D_{11}\alpha^4 + 2(D_{12} + 2D_{66})\alpha^2\beta^2 + D_{22}\beta^4, \ k_{45} = (Y_{13}^s + A_{55}^s)\alpha^2 + (Y_{23}^s + A_{44}^s)\beta^2$$
$$k_{34} = D_{11}^s\alpha^4 + 2(D_{12}^s + 2D_{66}^s)\alpha^2\beta^2 + D_{22}^s\beta^4, \ k_{55} = A_{55}^s\alpha^2 + A_{44}^s\beta^2 + Z_{33} \tag{20}$$
$$k_{35} = Y_{13}\alpha^2 + Y_{23}\beta^2, \ k_{44} = H_{11}\alpha^4 + 2(H_{12} + 2H_{66})\alpha^2\beta^2 + H_{22}\beta^4 + A_{55}^s\alpha^2 + A_{44}^s\beta^2$$
$$m_{11} = I_0, \ m_{13} = -\alpha I_1, \ m_{14} = -\alpha J_1, \ m_{22} = I_0, \ m_{23} = -\beta I_1, \ m_{24} = -\beta J_1$$
$$m_{33} = I_0 + I_2(\alpha^2 + \beta^2), \ m_{34} = I_0 + J_1(\alpha^2 + \beta^2), \ m_{35} = J_0$$
$$m_{44} = I_0 + K_2(\alpha^2 + \beta^2), \ m_{45} = J_0, \ m_{55} = K_0$$

4. Numerical results

4.1. Results for bending analysis

Consider a simply supported FG plate subjected to sinusoidal loads. The effective Young's modulus $E(z)$ is assumed to vary exponentially through the thickness of the plate as [33]

$$E(z) = E_0 \overline{f}(z), \ \overline{f}(z) = e^{p(0.5+z/h)} \tag{21}$$

where $E_b = E_0$ and $E_t = E_0 e^p$ denote Young's modulus of the bottom and top surfaces of the FG plate, respectively; E_0 is Young's modulus of the homogeneous plate; and p is a parameter that indicates the material variation through the thickness and takes values greater than or equal to zero. The variation of the exponential function $\bar{f}(z)$ through the thickness of the plate is presented in Fig. 1 for different values of p. Poisson's ratio is assumed to be constant $v = 0.3$. For convenience, the following dimensionless forms are used:

$$\bar{u}(z) = \frac{10E_0 h^3}{q_0 a^4} u\left(0, \frac{b}{2}, z\right), \quad \bar{w}(z) = \frac{10E_0 h^3}{q_0 a^4} w\left(\frac{a}{2}, \frac{b}{2}, z\right)$$

$$\bar{\sigma}_{x,y}(z) = \frac{h^2}{q_0 a^2} \sigma_{x,y}\left(\frac{a}{2}, \frac{b}{2}, z\right), \quad \bar{\sigma}_{xy}(z) = \frac{10h^2}{q_0 a^2} \sigma_{xy}(0, 0, z) \qquad (22)$$

$$\bar{\sigma}_{xz}(z) = \frac{h}{q_0 a} \sigma_{xz}\left(0, \frac{b}{2}, z\right), \quad \bar{\sigma}_{yz}(z) = \frac{h}{q_0 a} \sigma_{yz}\left(\frac{a}{2}, 0, z\right)$$

The dimensionless displacement and stress are presented in Tables 1-4 for various values of aspect ratio b/a, thickness ratio a/h, and material parameter p. The through thickness variations of the dimensionless displacements and stresses are also given in Fig. 2 for a thick FG plates with $a/h = 4$ and $p = 0.5$. The obtained results are compared with the exact 3D [33] and quasi-3D solutions [28,33-34]. It should be noted that the quasi-3D solutions [33-34] are derived based on a trigonometric variation of both in-plane and transverse displacements, while the quasi-3D solutions [28] are computed based on a cubic variation of in-plane displacements and a parabolic variation of transverse displacement across the thickness. In addition, the results of HSDT [35] are also provided to show the importance of including the thickness stretching effect. The HSDT solution [35] is computed based on a trigonometric variation of in-plane displacements and a constant transverse displacement across the thickness (i.e.,

thickness stretching effect is omitted, $\varepsilon_z = 0$).

It can be observed that the obtained results are in excellent agreement with 3D and quasi-3D solutions, particularly with those reported by Mantari and Guedes Soares [28,34]. The present quasi-3D theory is even more accurate than the quasi-3D sinusoidal theory [33]. Since the present quasi-3D theory and other quasi-3D theories include the thickness stretching effect, their solutions are very close to each other. Meanwhile, the HSDT [35], which omits this effect, gives inaccurate prediction and slightly overestimates the deflection especially for very thick plates (i.e., $a/h = 2$, see Tables 1 and 3). The errors in the HSDT are reduced with increasing the thickness ratio a/h. In general, the present quasi-3D theory is highly accurate and comparable to 3D solution even in the case of very thick plates, e.g., $a/h = 2$. It is worth noting that the developed theory consists of five unknowns, while the number of unknowns in the HSDT [35] and other quasi-3D theories [28,33-34] is five and six, respectively. Consequently, it may be concluded that the present quasi-3D theory is not only more accurate than the HSDT having the same five unknowns, but also comparable with the quasi-3D theories having more number of unknowns.

4.2. Results for free vibration analysis

The accuracy of the proposed quasi-3D theory is also verified through the free vibration analysis. Consider a simply supported Al/ZrO$_2$ plate made from a mixture of a metal (Al) and a ceramic (ZrO$_2$). Young's modulus and density of the metal are $E_m = 70\,\text{GPa}$ and $\rho_m = 2702\,\text{kg/m}^3$, respectively, and that of ceramic are $E_c = 380\,\text{GPa}$ and $\rho_c = 3800\,\text{kg/m}^3$, respectively. Poisson's ratio is assumed to be constant and equal to 0.3. The effective Young's modulus is estimated using the power-law distribution with Mori-Tanaka scheme. According to the power-law distribution with Mori-Tanaka

13

scheme, the bulk modulus $K(z)$ is given by [36]

$$K(z) = K_m + (K_c - K_m)\frac{V_c}{1 + V_m \frac{K_c - K_m}{K_m + 4/3G_m}} \tag{23}$$

where subscripts m and c represent the metal and ceramic constituents, respectively; G is the shear modulus; and the volume fractions of the metal phase V_m and ceramic phase V_c are given by

$$V_m = 1 - V_c \text{ and } V_c = (0.5 + z/h)^p \tag{24}$$

with p being the power law index. The variation of the volume fraction V_c through the thickness of the plate is given in Fig. 3 for various values of the power law index p. Recall that the bulk modulus and the shear modulus are related to Young's modulus E and Poisson ratio v by $K = E/3(1-2v)$ and $G = E/2(1+v)$. Thus, by rewriting Eq. (23) in terms of E and v, the effective Young's modulus $E(z)$ is rewritten by

$$E(z) = E_m + (E_c - E_m)\frac{V_c}{1 + V_m \left(\frac{E_c}{E_m} - 1\right)\frac{1+v}{3-3v}} \tag{25}$$

The effective density $\rho(z)$ is estimated using the power-law distribution with Voigt's rule of mixtures as [10]

$$\rho(z) = \rho_m + (\rho_c - \rho_m)V_c \tag{26}$$

Table 5 contains the dimensionless fundamental frequency $\bar{\omega}$ of square plates for different values of thickness ratio and power law index. The dimensionless frequency is defined by $\bar{\omega} = \omega h \sqrt{\rho_m / E_m}$. The calculated frequencies are compared with 3D solutions of Vel and Batra [37], quasi-3D solutions of Neves et al. [27,26,24], and third-order shear deformation (TSDT) solutions of Ferreira et al. [12]. It should be noted that

14

the quasi-3D solutions are derived based on the sinusoidal [26], hyperbolic [27], and cubic [24] variations of the in-plane displacements, and a quadratic variation of the transverse displacement across the thickness. Since the proposed and quasi-3D theories include the thickness stretching effect, they lead to solutions close to each other, and their solutions match well with 3D solution [37]. Whereas, the TSDT solutions [12] slightly underestimates frequency due to ignoring the thickness stretching effect. Again, it shoud be noted that the number of unknowns of the proposed theory is only five as against nine in the case of the quasi-3D theories of Neves et al. [27,26,24].

5. Conclusions

A quasi-3D hyperbolic shear deformation theory is developed for bending and vibration analysis of FG plates. The approach contains five unknowns, but accounts for both shear deformation and thickness stretching effects without the need for any shear correction factor. Equations of motion derived from Hamilton principle are analytically solved for bending and free vibration problems of a simply supported plate. By dividing the transverse displacement into the bending and shear parts, the number of unknowns of the theory is reduced, and the computational time is thus saved. The following main points may be drawn from the present study:

(1) The results predicted by the proposed theory are in an excellent agreement with 3D solutions even for the case of very thick plates with $a/h = 2$.

(2) The present quasi-3D theory has five unknowns, but gives results comparable with those predicted by the existing quasi-3D theories having more number of unknowns.

(3) The proposed theory is even more accurate than the quasi-3D sinusoidal theory when compared to 3D solution.

(4) The thickness stretching effect is more pronounced for thick plates and it needs to

15

be taken in consideration in the modeling.

References

1. Nguyen, T.K., Sab, K., Bonnet, G.: First-order shear deformation plate models for functionally graded materials. Compos. Struct. **83**(1), 25-36 (2008).

2. Zhao, X., Lee, Y.Y., Liew, K.M.: Free vibration analysis of functionally graded plates using the element-free kp-Ritz method. J. Sound Vib. **319**(3-5), 918-939 (2009).

3. Hosseini-Hashemi, S., Rokni Damavandi Taher, H., Akhavan, H., Omidi, M.: Free vibration of functionally graded rectangular plates using first-order shear deformation plate theory. Appl. Math. Modell. **34**(5), 1276-1291 (2010).

4. Hosseini-Hashemi, S., Fadaee, M., Atashipour, S.R.: A new exact analytical approach for free vibration of Reissner-Mindlin functionally graded rectangular plates. Int. J. Mech. Sci. **53**(1), 11-22 (2011).

5. Irschik, H.: On vibrations of layered beams and plates. J. Appl. Math. Mech. **73**(4-5), 34-45 (1993).

6. Nosier, A., Fallah, F.: Reformulation of Mindlin–Reissner governing equations of functionally graded circular plates. Acta Mech. **198**(3-4), 209-233 (2008).

7. Saidi, A.R., Baferani, A.H., Jomehzadeh, E.: Benchmark solution for free vibration of functionally graded moderately thick annular sector plates. Acta Mech. **219**(3-4), 309-335 (2011).

8. Yang, B., Ding, H.J., Chen, W.Q.: Elasticity solutions for a uniformly loaded rectangular plate of functionally graded materials with two opposite edges simply supported. Acta Mech. **207**(3-4), 245-258 (2009).

9. Zenkour, A.M., Allam, M.N.M., Shaker, M.O., Radwan, A.F.: On the simple and mixed first-order theories for plates resting on elastic foundations. Acta Mech. **220**(1-4), 33-46 (2011).

10. Reddy, J.N.: Analysis of functionally graded plates. Int. J. Numer. Methods Eng. **47**(1-3), 663-684 (2000).

11. Ferreira, A.J.M., Batra, R.C., Roque, C.M.C., Qian, L.F., Martins, P.A.L.S.: Static analysis of functionally graded plates using third-order shear deformation theory and a meshless method. Compos. Struct. **69**(4), 449-457 (2005).

12. Ferreira, A.J.M., Batra, R.C., Roque, C.M.C., Qian, L.F., Jorge, R.M.N.: Natural frequencies of functionally graded plates by a meshless method. Composite Structures **75**(1-4), 593-600 (2006).

13. Zenkour, A.M.: Generalized shear deformation theory for bending analysis of functionally graded plates. Appl. Math. Modell. **30**(1), 67-84 (2006).

14. Pradyumna, S., Bandyopadhyay, J.N.: Free vibration analysis of functionally graded curved panels using a higher-order finite element formulation. J. Sound Vib. **318**(1-2), 176-192 (2008).

15. Bodaghi, M., Saidi, A.R.: Levy-type solution for buckling analysis of thick functionally graded rectangular plates based on the higher-order shear deformation plate theory. Applied Mathematical Modelling **34**(11), 3659-3673 (2010).

16. Hosseini-Hashemi, S., Fadaee, M., Atashipour, S.R.: Study on the free vibration of thick functionally graded rectangular plates according to a new exact closed-form

procedure. Compos. Struct. **93**(2), 722-735 (2011).

17. Xiang, S., Jin, Y.X., Bi, Z.Y., Jiang, S.X., Yang, M.S.: A n-order shear deformation theory for free vibration of functionally graded and composite sandwich plates. Compos. Struct. **93**(11), 2826-2832 (2011).

18. Qian, L.F., Batra, R.C., Chen, L.M.: Static and dynamic deformations of thick functionally graded elastic plates by using higher-order shear and normal deformable plate theory and meshless local Petrov–Galerkin method. Composites Part B **35**(6–8), 685-697 (2004).

19. Carrera, E., Brischetto, S., Cinefra, M., Soave, M.: Effects of thickness stretching in functionally graded plates and shells. Composites Part B **42**(2), 123-133 (2011).

20. Kant, T., Swaminathan, K.: Analytical solutions for the static analysis of laminated composite and sandwich plates based on a higher order refined theory. Compos. Struct. **56**(4), 329-344 (2002).

21. Chen, C.S., Hsu, C.Y., Tzou, G.J.: Vibration and stability of functionally graded plates based on a higher-order deformation theory. J. Reinf. Plast. Compos. **28**(10), 1215-1234 (2009).

22. Talha, M., Singh, B.N.: Static response and free vibration analysis of FGM plates using higher order shear deformation theory. Appl. Math. Modell. **34**(12), 3991-4011 (2010).

23. Reddy, J.N.: A general nonlinear third-order theory of functionally graded plates. Int. J. Aerosp. Lightweight Struct. **1**(1), 1-21 (2011).

24. Neves, A.M.A., Ferreira, A.J.M., Carrera, E., Cinefra, M., Roque, C.M.C., Jorge, R.M.N., Soares, C.M.M.: Static, free vibration and buckling analysis of isotropic and sandwich functionally graded plates using a quasi-3D higher-order shear

deformation theory and a meshless technique. Composites Part B **44**(1), 657-674 (2013).

25. Ferreira, A.J.M., Carrera, E., Cinefra, M., Roque, C.M.C., Polit, O.: Analysis of laminated shells by a sinusoidal shear deformation theory and radial basis functions collocation, accounting for through-the-thickness deformations. Composites Part B **42**(5), 1276-1284 (2011).

26. Neves, A.M.A., Ferreira, A.J.M., Carrera, E., Roque, C.M.C., Cinefra, M., Jorge, R.M.N., Soares, C.M.M.: A quasi-3D sinusoidal shear deformation theory for the static and free vibration analysis of functionally graded plates. Composites Part B **43**(2), 711-725 (2012).

27. Neves, A.M.A., Ferreira, A.J.M., Carrera, E., Cinefra, M., Roque, C.M.C., Jorge, R.M.N., Soares, C.M.M.: A quasi-3D hyperbolic shear deformation theory for the static and free vibration analysis of functionally graded plates. Compos. Struct. **94**(5), 1814-1825 (2012).

28. Mantari, J.L., Guedes Soares, C.: Generalized hybrid quasi-3D shear deformation theory for the static analysis of advanced composite plates. Compos. Struct. **94**(8), 2561-2575 (2012).

29. Soldatos, K.P.: A transverse shear deformation theory for homogeneous monoclinic plates. Acta Mech. **94**(3), 195-220 (1992).

30. Xiang, S., Wang, K.M., Ai, Y.T., Sha, Y.D., Shi, H.: Analysis of isotropic, sandwich and laminated plates by a meshless method and various shear deformation theories. Compos. Struct. **91**(1), 31-37 (2009).

31. Akavci, S.: Two new hyperbolic shear displacement models for orthotropic laminated composite plates. Mech. Compos. Mater. **46**(2), 215-226 (2010).

32. El Meiche, N., Tounsi, A., Ziane, N., Mechab, I., Adda.Bedia, E.A.: A new hyperbolic shear deformation theory for buckling and vibration of functionally graded sandwich plate. Int. J. Mech. Sci. **53**(4), 237-247 (2011).

33. Zenkour, A.: Benchmark trigonometric and 3-D elasticity solutions for an exponentially graded thick rectangular plate. Arch. Appl. Mech. **77**(4), 197-214 (2007).

34. Mantari, J.L., Guedes Soares, C.: A novel higher-order shear deformation theory with stretching effect for functionally graded plates. Composites Part B **45**(1), 268-281 (2013).

35. Mantari, J.L., Guedes Soares, C.: Bending analysis of thick exponentially graded plates using a new trigonometric higher order shear deformation theory. Compos. Struct. **94**(6), 1991-2000 (2012).

36. Mori, T., Tanaka, K.: Average stress in matrix and average elastic energy of materials with misfitting inclusions. Acta Metall. **21**(5), 571-574 (1973).

37. Vel, S.S., Batra, R.C.: Three-dimensional exact solution for the vibration of functionally graded rectangular plates. J. Sound Vib. **272**(3-5), 703-730 (2004).

Figure Captions

Fig. 1. Variation of exponential function $\bar{f}(z)$ through the thickness of a FG plate for various values of parameter p

Fig. 2. Variation of dimensionless displacement and stresses through the thickness of plates ($a/h = 4$, $p = 0.5$)

Fig. 3. Variation of volume fraction V_c through the thickness of the plate for various values of the power law index p

Table Captions

Table 1. Dimensionless deflection $\bar{w}(0)$ of plates ($a/h = 2$)

Table 2. Dimensionless deflection $\bar{w}(0)$ of plates ($a/h = 4$)

Table 3. Dimensionless stress $\bar{\sigma}_y(h/2)$ of plates ($a/h = 2$)

Table 4. Dimensionless stress $\bar{\sigma}_y(h/2)$ of plates ($a/h = 4$)

Table 5. Dimensionless fundamental frequency $\bar{\omega}$ of square plates
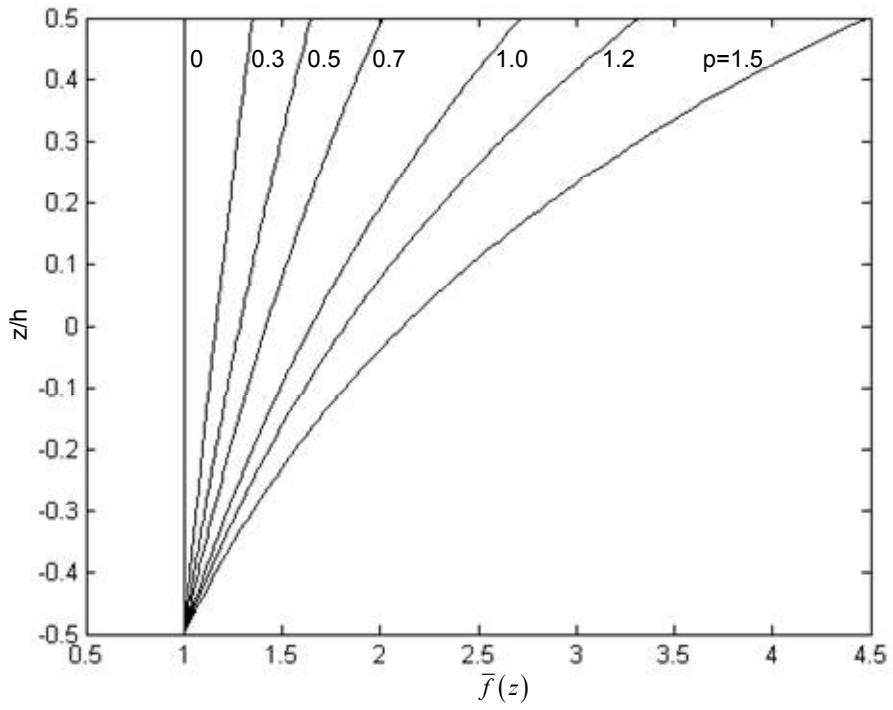
Fig. 1. Variation of exponential function $\bar{f}(z)$ through the thickness of a FG plate for various values of parameter p
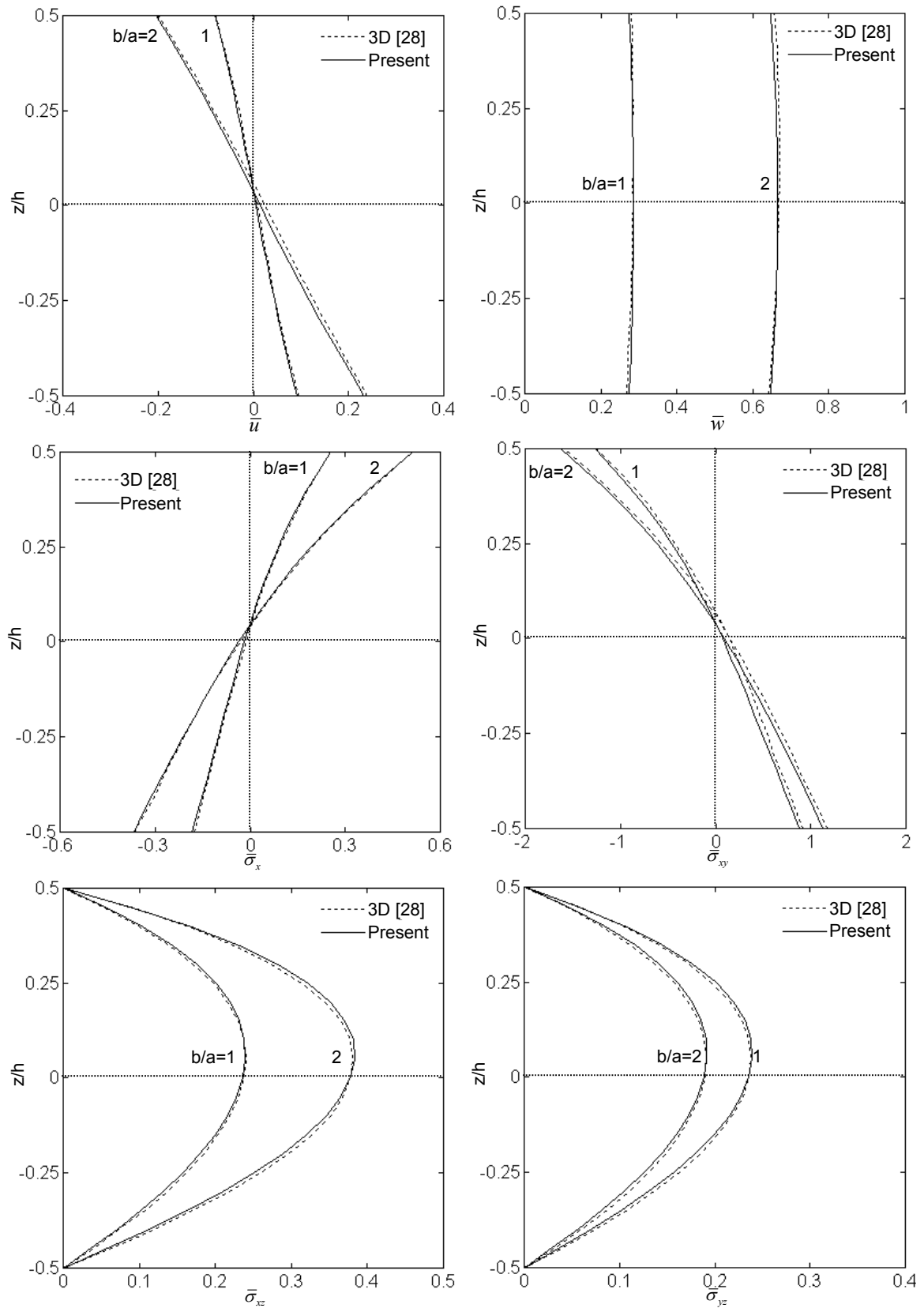
Fig. 2. Variation of dimensionless displacement and stresses through the thickness of plates ($a/h = 4$, $p = 0.5$)
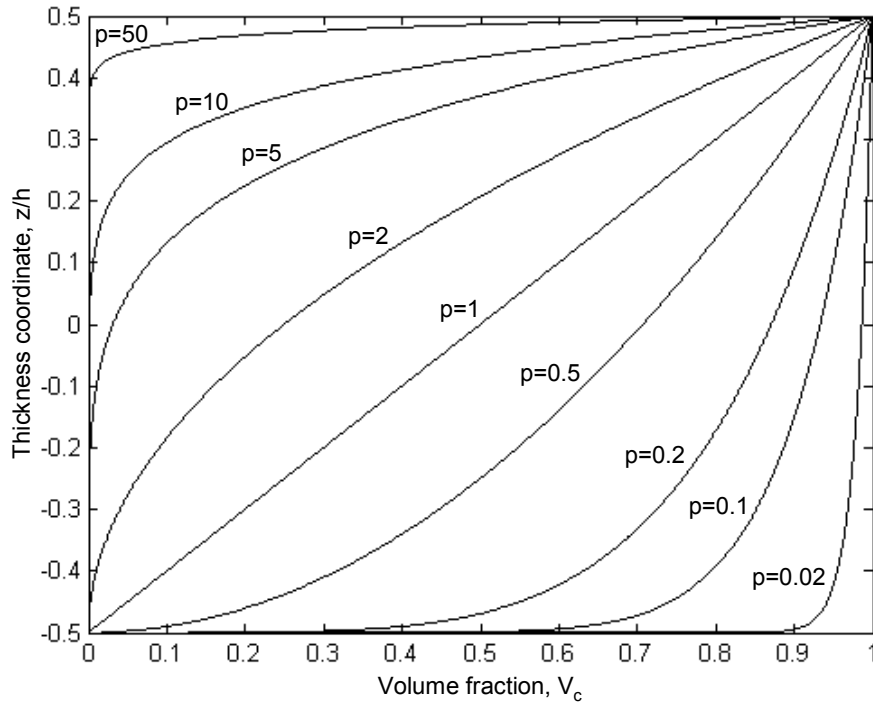
Fig. 3. Variation of volume fraction V_c through the thickness of the plate for various values of the power law index p

Table 1. Dimensionless deflection $\bar{w}(0)$ of plates ($a/h = 2$)

b/a	Methods	p					
		0.1	0.3	0.5	0.7	1.0	1.5
6	3D [33]	1.6377	1.4885	1.3518	1.2269	1.0593	0.8261
	quasi-3D [33]	1.6294	1.4731	1.3307	1.2010	1.0282	0.7906
	quasi-3D [34]	1.6365	1.4795	1.3364	1.2062	1.0333	0.7939
	Present	1.6367	1.4796	1.3365	1.2063	1.0327	0.7939
	HSDT [35]	1.7347	1.5688	1.4182	1.2815	1.1003	0.8500
5	3D [33]	1.6065	1.4601	1.3261	1.2035	1.0391	0.8102
	quasi-3D [33]	1.5983	1.4449	1.3052	1.1780	1.0086	0.7754
	quasi-3D [34]	1.6053	1.4513	1.3109	1.1832	1.0135	0.7787
	Present	1.6054	1.4514	1.3110	1.1833	1.0130	0.7787
	HSDT [35]	1.7025	1.5397	1.3919	1.2576	1.0798	0.8340
4	3D [33]	1.5515	1.4101	1.2807	1.1624	1.0035	0.7824
	quasi-3D [33]	1.5435	1.3954	1.2605	1.1376	0.9740	0.7487
	quasi-3D [34]	1.5504	1.4017	1.2661	1.1427	0.9788	0.7520
	Present	1.5505	1.4018	1.2662	1.1428	0.9783	0.7520
	HSDT [35]	1.6458	1.4885	1.3455	1.2157	1.0437	0.8060
3	3D [33]	1.4430	1.3116	1.1913	1.0812	0.9334	0.7275
	quasi-3D [33]	1.4354	1.2977	1.1722	1.0579	0.9057	0.6962
	quasi-3D [34]	1.4421	1.3037	1.1776	1.0628	0.9104	0.6993
	quasi-3D [28]	1.4419	1.3035	1.1774	1.0626	0.9096	0.6991
	Present	1.4422	1.3038	1.1777	1.0629	0.9098	0.6993
	HSDT [35]	1.5341	1.3784	1.2540	1.1329	0.9725	0.7506
2	3D [33]	1.1945	1.0859	0.9864	0.8952	0.7727	0.6017
	quasi-3D [33]	1.1880	1.0740	0.9701	0.8755	0.7494	0.5758
	quasi-3D [34]	1.1941	1.0795	0.9750	0.8799	0.7538	0.5786
	quasi-3D [28]	1.1938	1.0793	0.9748	0.8797	0.7530	0.5785
	Present	1.1942	1.0796	0.9751	0.8800	0.7532	0.5786
	HSDT [35]	1.2776	1.1553	1.0441	0.9431	0.8093	0.6238
1	3D [33]	0.5769	0.5247	0.4766	0.4324	0.3727	0.2890
	quasi-3D [33]	0.5731	0.5181	0.4679	0.4222	0.3612	0.2771
	quasi-3D [34]	0.5779	0.5224	0.4718	0.4257	0.3649	0.2794
	quasi-3D [28]	0.5776	0.5222	0.4716	0.4255	0.3640	0.2792
	Present	0.5780	0.5225	0.4719	0.4258	0.3642	0.2794
	HSDT [35]	0.6363	0.5752	0.5195	0.4687	0.4018	0.3079

Table 2. Dimensionless deflection $\overline{w}(0)$ of plates ($a/h = 4$)

b/a	Methods	p					
		0.1	0.3	0.5	0.7	1.0	1.5
6	3D [33]	1.1714	1.0622	0.9633	0.8738	0.7550	0.5919
	quasi-3D [33]	1.1668	1.0551	0.9535	0.8611	0.7382	0.5697
	quasi-3D [34]	1.1703	1.0583	0.9563	0.8636	0.7403	0.5713
	Present	1.1703	1.0583	0.9563	0.8636	0.7403	0.5713
	HSDT [35]	1.1920	1.0789	0.9767	0.8844	0.7623	0.5955
5	3D [33]	1.1459	1.0391	0.9424	0.8548	0.7386	0.5790
	quasi-3D [33]	1.1414	1.0321	0.9327	0.8423	0.7221	0.5573
	quasi-3D [34]	1.1448	1.0352	0.9355	0.8448	0.7242	0.5588
	Present	1.1448	1.0352	0.9354	0.8448	0.7242	0.5588
	HSDT [35]	1.1663	1.0556	0.9556	0.8653	0.7458	0.5825
4	3D [33]	1.1012	0.9985	0.9056	0.8215	0.7098	0.5564
	quasi-3D [33]	1.0968	0.9918	0.8963	0.8094	0.6939	0.5355
	quasi-3D [34]	1.1001	0.9948	0.8989	0.8118	0.6959	0.5370
	Present	1.1001	0.9948	0.8989	0.8118	0.6959	0.5370
	HSDT [35]	1.1211	1.0147	0.9186	0.8317	0.7169	0.5599
3	3D [33]	1.0134	0.9190	0.8335	0.7561	0.6533	0.5121
	quasi-3D [33]	1.0094	0.9127	0.8248	0.7449	0.6385	0.4927
	quasi-3D [34]	1.0124	0.9155	0.8272	0.7470	0.6404	0.4941
	quasi-3D [28]	1.0124	0.9155	0.8272	0.7470	0.6404	0.4941
	Present	1.0124	0.9155	0.8272	0.7470	0.6404	0.4941
	HSDT [35]	1.0325	0.9345	0.8459	0.7659	0.6601	0.5154
2	3D [33]	0.8153	0.7395	0.6707	0.6085	0.5257	0.4120
	quasi-3D [33]	0.8120	0.7343	0.6635	0.5992	0.5136	0.3962
	quasi-3D [34]	0.8145	0.7365	0.6655	0.6009	0.5151	0.3973
	quasi-3D [28]	0.8145	0.7365	0.6655	0.6009	0.5151	0.3973
	Present	0.8145	0.7365	0.6655	0.6009	0.5151	0.3973
	HSDT [35]	0.8325	0.7534	0.6819	0.6173	0.5319	0.4150
1	3D [33]	0.3490	0.3167	0.2875	0.2608	0.2253	0.1805
	quasi-3D [33]	0.3475	0.3142	0.2839	0.2563	0.2196	0.1692
	quasi-3D [34]	0.3486	0.3152	0.2848	0.2571	0.2203	0.1697
	quasi-3D [28]	0.3486	0.3152	0.2848	0.2571	0.2203	0.1697
	Present	0.3486	0.3152	0.2848	0.2571	0.2203	0.1697
	HSDT [35]	0.3602	0.3259	0.2949	0.2668	0.2295	0.1785

Table 3. Dimensionless stress $\bar{\sigma}_y\left(h/2\right)$ of plates ($a/h = 2$)

b/a	Methods	p					
		0.1	0.3	0.5	0.7	1.0	1.5
6	3D [33]	0.2943	0.3101	0.3270	0.3451	0.3746	0.4305
	quasi-3D [33]	0.2912	0.3118	0.3339	0.3573	0.3955	0.4679
	quasi-3D [34]	0.2763	0.2954	0.3159	0.3378	0.3737	0.4416
	Present	0.2759	0.2951	0.3155	0.3374	0.3730	0.4411
	HSDT [35]	0.2187	0.2345	0.2512	0.2690	0.2980	0.3498
5	3D [33]	0.2967	0.3128	0.3299	0.3483	0.3782	0.4350
	quasi-3D [33]	0.2935	0.3144	0.3366	0.3603	0.3988	0.4719
	quasi-3D [34]	0.2789	0.2983	0.3191	0.3412	0.3776	0.4461
	Present	0.2786	0.2980	0.3187	0.3408	0.3768	0.4456
	HSDT [35]	0.2219	0.2378	0.2548	0.2729	0.3024	0.3549
4	3D [33]	0.3008	0.3173	0.3349	0.3537	0.3844	0.4426
	quasi-3D [33]	0.2974	0.3186	0.3412	0.3653	0.4045	0.4786
	quasi-3D [34]	0.2834	0.3032	0.3243	0.3469	0.3839	0.4537
	Present	0.2830	0.3028	0.3239	0.3465	0.3832	0.4532
	HSDT [35]	0.2272	0.2435	0.2610	0.2795	0.3097	0.3634
3	3D [33]	0.3081	0.3252	0.3436	0.3633	0.3953	0.4562
	quasi-3D [33]	0.3042	0.3261	0.3493	0.3741	0.4143	0.4904
	quasi-3D [34]	0.2912	0.3118	0.3337	0.3571	0.3954	0.4673
	quasi-3D [28]	0.2920	0.3127	0.3347	0.3582	0.3963	0.4688
	Present	0.2909	0.3114	0.3333	0.3567	0.3947	0.4668
	HSDT [35]	0.2368	0.2539	0.2721	0.2914	0.3230	0.3788
2	3D [33]	0.3200	0.3385	0.3583	0.3796	0.4142	0.4799
	quasi-3D [33]	0.3146	0.3376	0.3620	0.3880	0.4300	0.5092
	quasi-3D [34]	0.3042	0.3261	0.3495	0.3743	0.4148	0.4905
	quasi-3D [28]	0.3049	0.3269	0.3503	0.3752	0.4155	0.4918
	Present	0.3040	0.3259	0.3492	0.3740	0.4142	0.4901
	HSDT [35]	0.2539	0.2723	0.2919	0.3128	0.3469	0.4064
1	3D [33]	0.3103	0.3292	0.3495	0.3713	0.4067	0.4741
	quasi-3D [33]	0.2955	0.3181	0.3421	0.3675	0.4085	0.4851
	quasi-3D [34]	0.2924	0.3147	0.3383	0.3633	0.4041	0.4785
	quasi-3D [28]	0.2927	0.3149	0.3385	0.3636	0.4039	0.4790
	Present	0.2924	0.3146	0.3382	0.3632	0.4034	0.4783
	HSDT [35]	0.2943	0.3101	0.3270	0.3451	0.3746	0.4305

Table 4. Dimensionless stress $\bar{\sigma}_y(h/2)$ of plates ($a/h = 4$)

b/a	Methods	p					
		0.1	0.3	0.5	0.7	1.0	1.5
6	3D [33]	0.2181	0.2321	0.2470	0.2628	0.2886	0.3373
	quasi-3D [33]	0.2369	0.2520	0.2683	0.2857	0.3144	0.3699
	quasi-3D [34]	0.2127	0.2255	0.2393	0.2544	0.2795	0.3294
	Present	0.2121	0.2249	0.2387	0.2537	0.2787	0.3285
	HSDT [35]	0.2010	0.2149	0.2298	0.2455	0.2711	0.3192
5	3D [33]	0.2206	0.2348	0.2498	0.2659	0.2920	0.3413
	quasi-3D [33]	0.2391	0.2545	0.2710	0.2886	0.3176	0.3737
	quasi-3D [34]	0.2152	0.2283	0.2424	0.2577	0.2832	0.3337
	Present	0.2147	0.2277	0.2418	0.2570	0.2825	0.3328
	HSDT [35]	0.2037	0.2178	0.2329	0.2488	0.2747	0.3235
4	3D [33]	0.2247	0.2392	0.2546	0.2710	0.2977	0.3482
	quasi-3D [33]	0.2429	0.2586	0.2754	0.2934	0.3230	0.3800
	quasi-3D [34]	0.2196	0.2330	0.2475	0.2633	0.2894	0.3411
	Present	0.2190	0.2324	0.2469	0.2626	0.2887	0.3402
	HSDT [35]	0.2082	0.2226	0.2380	0.2544	0.2808	0.3307
3	3D [33]	0.2319	0.2469	0.2629	0.2800	0.3077	0.3602
	quasi-3D [33]	0.2493	0.2656	0.2831	0.3017	0.3323	0.3911
	quasi-3D [34]	0.2272	0.2414	0.2566	0.2731	0.3004	0.3540
	quasi-3D [28]	0.2286	0.2429	0.2583	0.2749	0.3024	0.3563
	Present	0.2267	0.2408	0.2560	0.2725	0.2997	0.3532
	HSDT [35]	0.2162	0.2312	0.2472	0.2642	0.2917	0.3435
2	3D [33]	0.2431	0.2591	0.2762	0.2943	0.3238	0.3797
	quasi-3D [33]	0.2588	0.2761	0.2946	0.3143	0.3464	0.4079
	quasi-3D [34]	0.2395	0.2550	0.2715	0.2894	0.3187	0.3756
	quasi-3D [28]	0.2407	0.2563	0.2730	0.2909	0.3204	0.3776
	Present	0.2391	0.2545	0.2710	0.2888	0.3181	0.3749
	HSDT [35]	0.2294	0.2454	0.2624	0.2805	0.3097	0.3647
1	3D [33]	0.2247	0.2399	0.2562	0.2736	0.3018	0.3588
	quasi-3D [33]	0.2346	0.2510	0.2684	0.2870	0.3171	0.3739
	quasi-3D [34]	0.2237	0.2391	0.2554	0.2729	0.3014	0.3556
	quasi-3D [28]	0.2244	0.2398	0.2563	0.2738	0.3024	0.3567
	Present	0.2235	0.2388	0.2551	0.2726	0.3010	0.3551
	HSDT [35]	0.2164	0.2316	0.2477	0.2649	0.2927	0.3451

Table 5. Dimensionless fundamental frequency $\bar{\omega}$ of square plates

Method	p=0		p=1			a/h=5		
	$a/h=\sqrt{10}$	a/h=10	a/h=5	a/h=10	a/h=20	p=2	p=3	p=5
3D [37]	0.4658	0.0578	0.2192	0.0596	0.0153	0.2197	0.2211	0.2225
Quasi-3D [26]	-	-	0.2193	0.0596	0.0153	0.2198	0.2212	0.2225
Quasi-3D [27]	-	-	0.2193	0.0596	0.0153	0.2201	0.2216	0.2230
Quasi-3D [24]	-	-	0.2193	-	-	0.2200	0.2215	0.2230
TSDT [12]	-	-	0.2188	0.0592	0.0147	0.2188	0.2202	0.2215
Present	0.4661	0.0578	0.2192	0.0597	0.0153	0.2201	0.2214	0.2225